JOURNAL OF GEOPHYSICAL RESEARCH, VOL. 103, NO. E5, PAGES 11,125–11,133, MAY 25, 1998

Water content of the Martian soil: Laboratory simulations of reflectance spectra

Albert S. Yen, Bruce C. Murray, and George R. Rossman
Division of Geological and Planetary Sciences, California Institute of Technology, Pasadena

Abstract. Reflectance spectra from the surface of Mars collected by instruments such as the imaging spectrometer (ISM) onboard the 1988 Soviet Phobos 2 spacecraft exhibit strong 3 μm absorption features that have long been attributed to hydrated materials on the Martian surface. This interpretation is consistent with a series of chemical weathering models suggesting an abundance of palagonites, clays, and other hydrated mineral phases in the Martian fines. Little work, however, has been done to constrain the actual water content of the Martian surface materials. New laboratory data presented here show that the ISM spectra are consistent with up to 4% water by weight and that the deep hydration features observed in the spacecraft data could be due to less than 0.5% water if the hydrated phases are present in the form of grain coatings. These results are consistent with the somewhat uncertain in situ measurements obtained by the Viking landers which yielded approximately 2 wt % water from samples heated to 500°C. On the basis of this work, we expect the TEGA instrument on the Mars '98 lander to find less than 4% adsorbed or bound water in the upper few centimeters of the Martian soil.

1. Introduction

1.1. Predictions of Hydrated Minerals on the Martian Surface

Geologic interpretations of spacecraft images indicate that liquid water was once abundant on the surface of Mars [*Carr*, 1996]. The availability of surface water early in Mars' history suggests that primary basaltic rocks and volcanic glasses could have been chemically altered to secondary, hydrated mineral phases in that time period. In particular, much published literature infers an abundance of palagonites on the surface on the basis of spectroscopic evidence, thermodynamic calculations, laboratory experiments, and models of basalt erupting through ice [*Soderblom and Wenner*, 1978; *Gooding and Keil*, 1978; *Allen et al.*, 1981; *Singer*, 1982; *Morris et al.*, 1990; *Bell et al.*, 1993]. Other authors contend that smectite clays dominate the Martian fine particles [*Toulmin et al.*, 1977; *Baird et al.*, 1977; *Zolotov et al.*, 1983; *Banin et al.*, 1983, 1992; *Bishop et al.*, 1993]. *Burns* [1988] argues that weathering models and visible spectral data are consistent with ferrihydrite, jarosite, opal, and silicate clays. The presence of iron oxyhydroxides also has been suggested [*Morris et al.*, 1983; *Banin et al.*, 1993; *Burns and Fisher*, 1993]. Such analyses and inferences about the mineralogy of the Martian surface suggest that numerous hydrated phases are plausibly present.

1.2. Strong OH Absorption in Near-IR Reflectance

Interpretations suggesting that hydrated minerals are present on the surface of Mars are consistent with the broad absorption centered around 3 μm that has been observed in reflectance spectra from Mars since the early 1960s. This feature has been attributed to the OH stretch of adsorbed, bound, or frozen water in surface materials [*Moroz*, 1964; *Sinton*, 1967; *Houck et al.*, 1973; *Pimentel et al.*, 1974; *Calvin*, 1997]. Spectra collected by the imaging spectrometer (ISM) onboard the Soviet Phobos 2 spacecraft indicate that 3-μm band depths as large as ~0.62 are seen in the Martian surface (S. Murchie et al., NIR spectral variations on Mars from ISM imaging spectrometer data: Evidence for lithological variations of the surface layer, submitted to *Icarus*, 1997, hereinafter referred to as Murchie et al., submitted manuscript, 1997). These ISM observations at high spatial resolution (~25 km) also detected regional variability of up to 20% in the depth of the 3-μm feature [*Bibring et al.*, 1990; *Erard et al.*, 1991]. This variability of the OH signature in the ISM data is consistent with the reflectance spectra obtained from the infrared spectrometers (IRS) on board Mariners 6 and 7 [*Erard and Calvin*, 1997]. The depths of the IRS absorptions measured at 3 μm, however, are ~15% larger than corresponding ISM data. This difference has been attributed primarily to the larger phase angles in the IRS observations, which result in more scattering in the continuum [*Erard and Calvin*, 1997; Murchie et al., submitted manuscript, 1997.]

1.3. In-Situ Analyses

The only direct measurement of the water content of the Martian surface materials was performed by the gas chromatograph–mass spectrometer (GC-MS) instrument on board the Viking landers. (Water (H_2O molecules) released from soil samples by heating can initially reside on the surfaces of soil grains (adsorbed), interlayer in clays, bound in mineral phases as H_2O, or held as OH within the structure. References to "water" content in this paper refer to all forms of hydration that result in the evolution of H_2O upon heating.) The results from one of the landers (VL-2) indicate that less than 2% water by weight was evolved from each of two samples heated in rapid (30 s) steps to 500°C [*Biemann et al.*, 1977]. The uncertainty in this value, however, is significant for the following reasons: (1) The instrument was not specifically designed to detect water; in fact, the GC column was constructed to allow water to pass quickly through the system so that it could be expelled prior to analysis of organic species. Laboratory sim-

Paper number 98JE00739.
0148-0227/98/98JE-00739$09.00

Table 1. Approximate Particle Size Distribution for Laboratory Samples

Particle Size Range, μm	Percentage of Mixture
<300	100
<150	65
<75	40
<35	20
<10	10

ulations were necessary to understand the mass chromatograms obtained from the flight instrument, and "in the very worst case could be off by a factor of 5" [*Biemann et al.*, 1977, p. 4655]. (2) A temperature of 500°C is insufficient to dehydroxylate certain phyllosilicates such as montmorillonite [*de Bruyn and van der Marel*, 1954]. (3) Adsorbed water could have been lost from the sample during exposure to the Martian atmosphere at elevated temperatures (15°C) within the lander prior to the analyses [*Anderson and Tice*, 1979]. Some authors even suggest that the Viking lander results "place virtually no constraints on the possible contents of hydrous minerals" in the Martian surface [*Arvidson et al.*, 1989, p. 52].

1.4. Focus of This Study

The purpose of this paper is to show that even with all the uncertainties, the 2% result obtained by the Viking landers is reasonable for the water content of the Martian soil. We demonstrate that the strong 3-μm absorption feature in the spacecraft reflectance spectra can be reproduced with plausible mineral mixtures containing less than 4% water by weight. Furthermore, we show that it is difficult to "hide" larger quantities of water in the Martian surface layer while maintaining reflectance spectra consistent with those collected from spacecraft.

1.5. Past Work

Houck et al. [1973] collected 3-μm spectra from an aircraft instrument similar in depth to the ISM results. They then estimated and inferred scattering coefficients for the Martian particulate surface and thereby constrained the water content of the soil to be approximately 1% (within a factor of 3). We use experimental rather than theoretical arguments, as well as more recent and much higher fidelity reflection spectra of Mars (ISM data) to show that the observed 3-μm absorption feature is consistent with Viking in situ measurements. We use the ISM and IRS spectra for comparison with our laboratory data because of the absence of terrestrial atmospheric interference and the high spatial resolution.

2. Experiment Description

2.1. Overview

Mars-analog soil samples of varied water content were prepared and scanned using a Fourier transform infrared (FTIR) spectrometer. Thermal gravimetry (TG) was used to confirm the water content of the samples. The laboratory data were subsequently compared with published ISM and IRS spectra.

2.2. Sample Preparation

The water- and OH-containing component of the particulate mixtures used in our experiments included palagonite, bentonite, goethite, and gypsum. The palagonite is the Pahala Ash from Hawaii (~3 km west of Naalehu on Highway 11). Bentonite is a weathered volcanic ash consisting of mostly montmorillonite; our samples are from Clay Spur, Wyoming (Clay Mineral Standard H-26). The goethite (α-FeOOH) sample is from Negaunee, Michigan, and the gypsum ($CaSO_4 \cdot 2H_2O$) is the selenite variety from Utah. The anhydrous portions of the mixtures included augite (clinopyroxene) from Ontario, Canada (near Syndenham); a fresh sample of Kilauea pahoehoe basalt; and near-gem-quality plagioclase feldspar (~An70) from the Ponderosa Mine in Oregon. Basalts are largely plagioclase feldspar, but the transparent samples from Ponderosa Mine were used because they lack the highly absorbing dark-colored minerals such as magnetite. The objective of this study is not to test all possible Martian surface constituents. Rather, samples were selected to be representative of the major categories of suspected mineral phases. Indeed, the results described below will show that the data depend primarily on water content and are relatively insensitive to the sample composition.

All of the samples were ground by hand using a mortar and pestle and dry sieved to exclude particles greater than 300 μm in diameter. Before the mixtures for FTIR analysis were made, the anhydrous components were baked at 850°C under air for 50 hours to minimize the adsorbed water. Neither the X ray diffraction patterns nor the mid-infrared characteristics (with the exception of the removal of the 3-μm absorption) of the samples were altered by baking. The visual appearance of the basalt and the augite, however, changed from their initial gray and greenish colors to a more reddish brown hue from thermal oxidation, which better resembles the visible color of Mars.

2.3. Particle Size Considerations

Martian soils are estimated to range from approximately 2 μm to 300 μm in particle size. Dust particles suspended in the Martian atmosphere have typical sizes of the order of 2.5 μm [*Pollack et al.*, 1979]. Particles that are most easily saltated by surface winds have diameters of approximately 100 μm [*Greeley et al.*, 1992]. An average particle size of 100 μm is also consistent with observations of the drifts of fine-grained sand in the vicinity of the Viking landers [*Sharp and Malin*, 1984]. Thermal inertia studies of aeolian deposits suggest an average particle size of 300 μm [*Palluconi and Kieffer*, 1981]. Because we wish to show the plausibility of duplicating the ISM spectra using reasonable choices for particle size, sample material, and water content, we use particle mixtures that are no larger than 300 μm.

The approximate size distribution of our samples is listed in Table 1. Sizes down to 35 μm were determined by sieving, and the fraction smaller than 10 μm was estimated by microscopic examination. The ISM instrument had a spatial resolution of ~25 km and undoubtedly sampled rocks, boulders, and other surfaces with length scales of the order of meters and larger. However, the roughness scale of most geologic surfaces combined with the sizes of aeolian material known to be on Mars indicate that surface spectra will be dominated by diffuse reflectance in the wavelength range studied here. This assumption facilitates a direct comparison between laboratory and spacecraft data.

2.4. Sample Characterization

Each of the samples used in this study was analyzed with X ray diffraction (XRD) to verify the composition. All powder

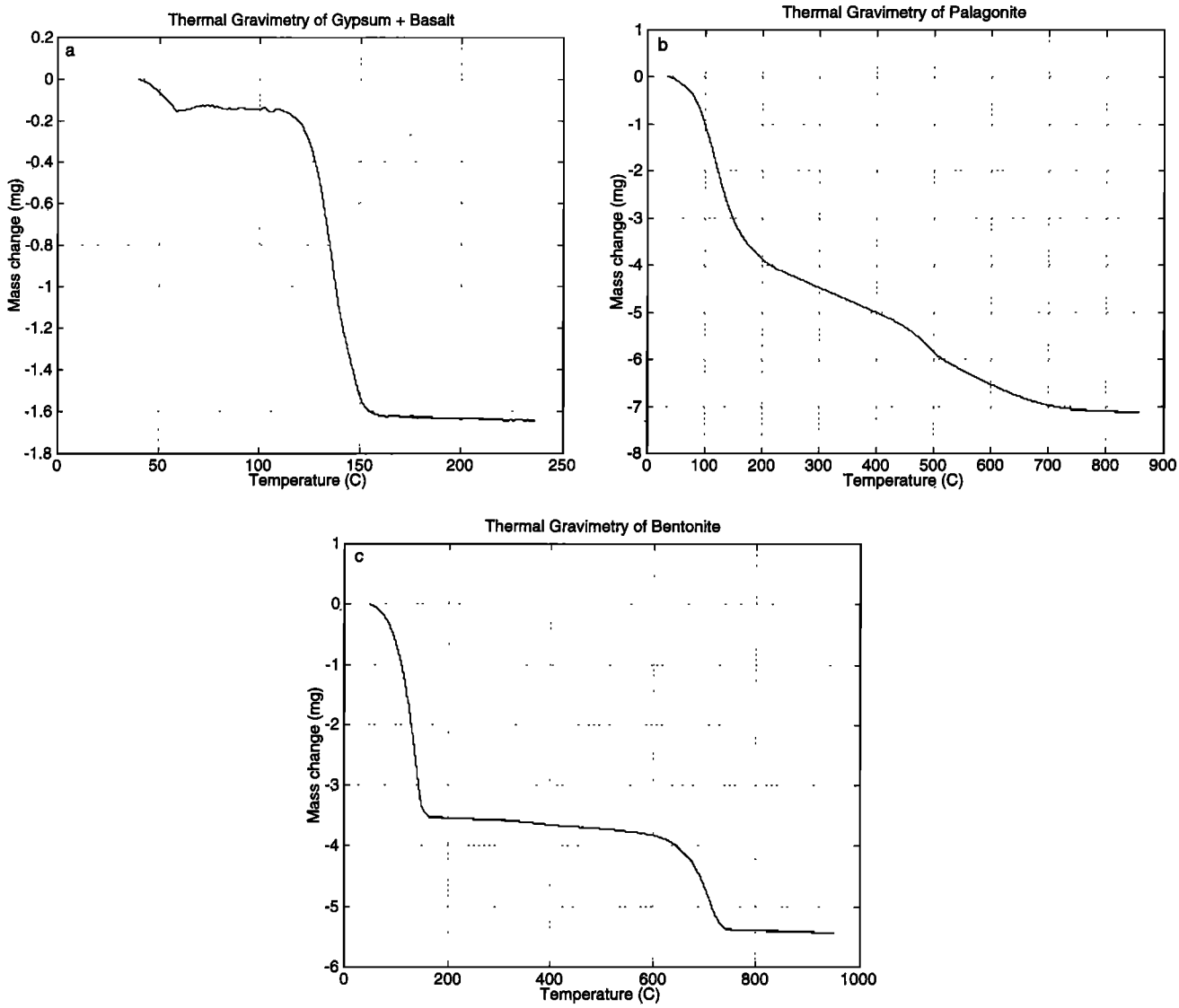

Figure 1. (a) Thermal gravimetry profile for a mixture of gypsum and basalt. The desired water content of this mixture was 2.0 wt %, which was confirmed experimentally with the loss of 1.64 mg from an 82.3-mg sample. (b) TG profile for Pahala Ash. A 7.1-mg mass loss from an initial sample of 38.4 mg indicates ~18.5 wt % water under the temperature and humidity conditions on the day of this thermal analysis. (c) TG profile for bentonite from Clay Spur, Wyoming. A 5.4-mg change in mass from a 46.4-mg sample corresponds to an initial water content of 11.6 wt % on the day of this experiment. Interlayer water is lost below 200°C, while structurally bound OH is lost from the montmorillonite near 700°C.

patterns are as expected: Goethite, gypsum, augite, and plagioclase clearly match the database patterns. Bentonite and palagonite samples are dominated by montmorillonite. The low signal level in the palagonite sample indicates that this weathering product of basaltic glass is poorly ordered and almost amorphous. The diffraction patterns obtained for the basalt samples are dominated by plagioclase feldspars.

2.5. Thermal Analysis of Water Content

Dry basalt, feldspar, and pyroxene were mixed with hydrated mineral phases for comparison with the ISM spectra. Values for the water content of goethite and gypsum were initially estimated from stochiometry as 10.1% and 20.9% water by weight, respectively. After mixtures containing 2%, 4%, 6%, and 8% water by weight were made and scanned in the FTIR as described below, portions of the sample were extracted for thermal analysis using a Mettler TA2000C Thermoanalyzer to confirm the water content. An example of a thermal gravimetry curve is shown in Figure 1a. The intended amount of water from gypsum in this particular example is 2.0% by weight. An 82.3-mg sample of the mixture was heated to 1000°C at 10°C min^{-1}, and the weight loss was measured as a function of temperature. The 1.64 mg of water lost as shown Figure 1a corresponds to 2.0% of the total mass, confirming the accuracy of our sample preparation.

Palagonite and bentonite are well known to adsorb large quantities of water (owing to high surface area and interlayer sites in the clays, primarily montmorillonite). Because the actual stochiometry is unknown and unreliable for determining the quantity of water in these hydrated phases, initial estimates of water content were obtained from the thermal analysis

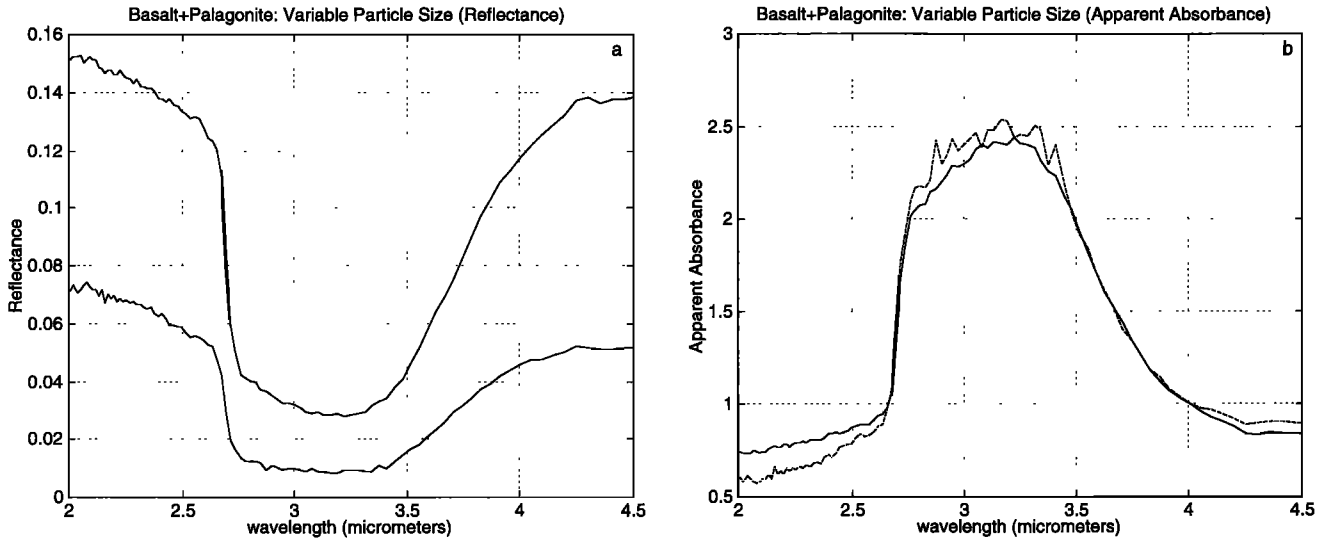

Figure 2. (a) Reflectance measurements for mixtures of palagonite and basalt. The upper curve represents particles less than 38 μm in size, while the lower curve is for particles between 75 and 150 μm (mixtures were made after sieving of individual components). (b) Conversion of the curves in Figure 2a to apparent absorbance ($-\ln(R)$) and superimposed for comparison. Absorbance is reproducible for constant water content and varying particle size, while reflectance band depths change with particle size. The dashed line represents particles between 75 and 150 μm, while the solid line represents particles less than 38 μm in size.

curves. Small (<50 mg) quantities heated to 1000°C at 10°C min^{-1} show that the palagonite and bentonite samples used in this study contain approximately 18.5% and 11.6% water by weight, respectively (see Figures 1b and 1c). Even though these samples are stored in sealed containers, exposure to variable humidity air during the sample preparation process affects the actual level of hydration. Thus analysis of the water content by these same thermal techniques immediately after collecting the infrared reflectance data was necessary to confirm that the desired water content was achieved.

2.6. Infrared Spectroscopy

After the powdered mixtures of baked basalt plus a hydrated phase were made (under air) and placed in sample cups, biconical diffuse reflectance spectra were obtained using a Nicolet 60SX FTIR spectrometer. The purge gas flowing into the analysis chamber of the instrument was air that had been pressure cycled through zeolite to remove water vapor and carbon dioxide. A reflectance standard manufactured by Labsphere (Infragold) was used as the reference; manufacturer's data indicate that 94–97% of the incident flux in the applicable wavelength range is reflected from the surface. The infrared beam from the interferometer is focused to a spot size of approximately 3 mm by an off-axis paraboloid mirror. This focal spot is significantly larger than the particle size of the samples and the ~50 μm feature size of the Infragold standard, which allows collection of the diffuse portion of the reflectance. Scans of the reference target immediately precede scans of the soil mixtures, and a ratio between the two data sets was computed to eliminate the spectral contribution of the optical path through the instrument. The resulting data represent the reflectance spectra of the sample from 2 μm to 5 μm.

2.7. Conversion to Absorbance

Quantitative analysis using only reflectance spectra poses several challenges. First, the effects of wavelength dependent scattering alter the relative depths of the absorption features for samples with the same bulk water content but different particle sizes and packing densities. Furthermore, because reflectance values relative to a suitable standard range between zero and one, doubling the water content will not double the size of the absorption band. A number of techniques have been described in the literature for converting reflectance to absorbance in an effort to account for scattering processes and to relieve the effects of logarithmic compression (see *Hapke* [1993] for a review). None of these techniques is ideally suited for our particular problem, but one of the less unsatisfactory approaches for linearizing the reflectance data from the laboratory (as well as the spacecraft) measurements is to use the "apparent absorbance" ($-\ln(R)$) [*Kortum*, 1969; *Clark and Roush*, 1984].

Reflectance band depths vary considerably as particle sizes and packing densities of the samples are varied in the laboratory. Our experiments show that variations as large as 50% are achievable from changes in particle size and packing density while water contents of the samples are constant. Conversion of these reflectances to apparent absorbance, however, yielded much smaller differences between samples (less than 10%). For example, Figures 2a and 2b show reflectance and absorbance, respectively, for mixtures of palagonite and basalt of different particle sizes. While the reflectance band depths are different for the same quantity of water, the absorbance curves are nearly identical. Similar results have been demonstrated with packing density variations. Thus conversion to apparent absorbance is robust to changes in packing density and particle size, and direct comparisons between curves of different quantities of water can be made after the conversion to absorbance is applied.

2.8. Results

Ten "families" of four curves such as the ones shown in Figures 3a through 3d were produced from these experiments.

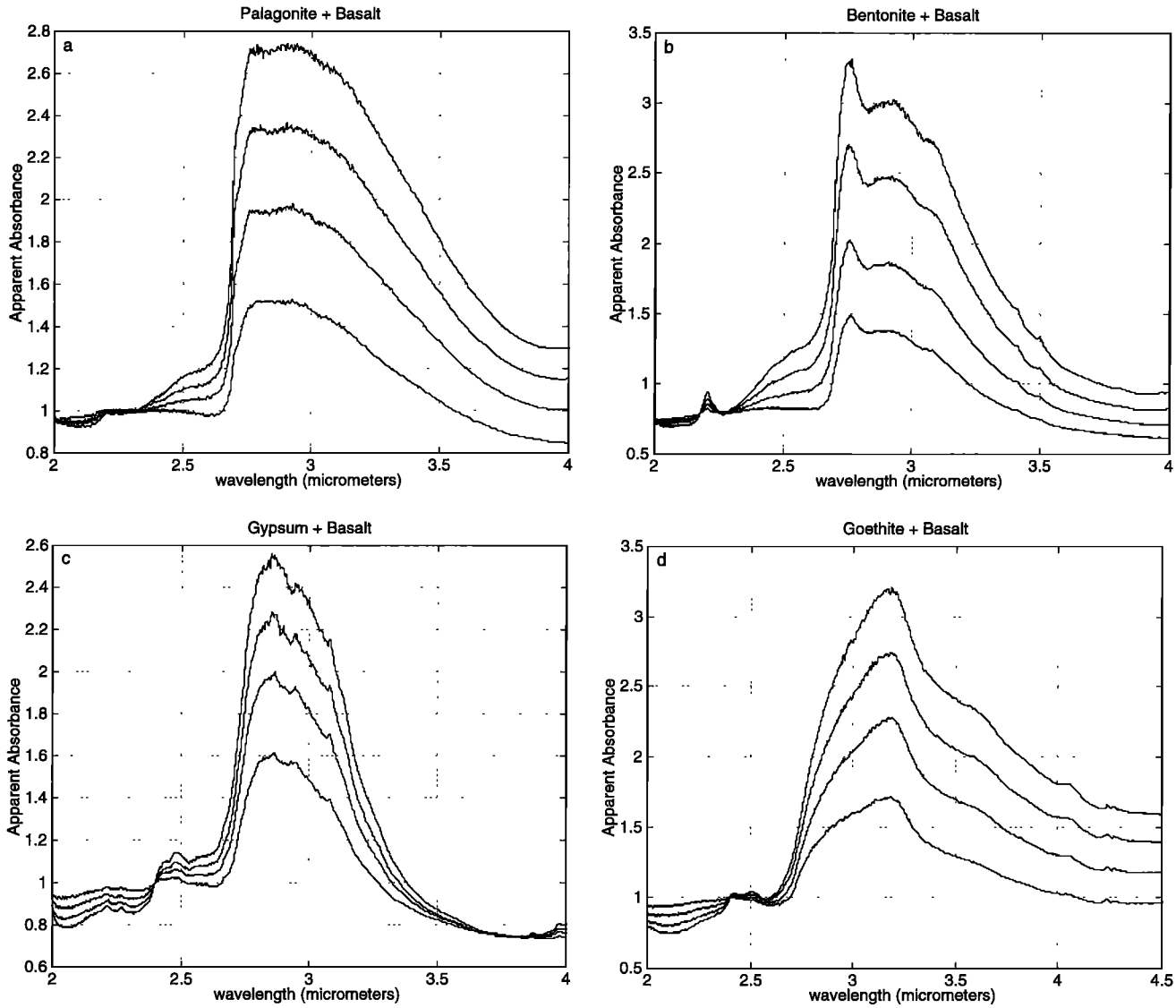

Figure 3. Example of increasing absorbance with larger water content for mixtures of basalt and (a) palagonite (b) bentonite, (c) gypsum, and (d) goethite (each component dry sieved to diameters less than 300 μm). Reflectance spectra are converted to apparent absorbance. Vertical axes are offset to align curves. Water content varies from 2% (lowest curve) to 8% (highest peak); intermediate curves represent 4% and 6% water.

One set of curves was generated for each combination of dry (basalt, feldspar, pyroxene) and hydrated mineral phases (palagonite, bentonite, gypsum), and the tenth plot was produced from a mixture of basalt and goethite. The four curves in each plot represent 2, 4, 6, and 8% water by weight. To simplify comparison across the data sets, the curves were reduced to apparent absorbance heights after an approximate continuum baseline was subtracted from the absorbance spectra. Plots of apparent absorbance versus water content for the various mixtures are shown in Figure 4a. The representative error bars in Figure 4a were estimated from FTIR and thermal analysis of multiple mixtures with the same target water content and by bounding the range of absorbance values for different choices for baseline corrections. In the bentonite curves, where the absorbance peak is at 2.76 μm, the second highest peak (~2.9 μm) was used to determine the band size. This region of the curve is more appropriate for a direct comparison with the ISM results, since the spacecraft data in the wavelength range of the largest peak are highly uncertain because of interference from atmospheric CO_2 (see discussion below).

3. Discussion

3.1. Comparison With Spacecraft Data

The instruments that provide the best data for comparison against the laboratory spectra are the infrared spectrometers on board Mariners 6 and 7 and the imaging spectrometer from the Soviet Phobos 2 spacecraft. An apparent advantage of the latter data set is that a number of authors have published ISM spectra covering the 3-μm absorption feature that have been "corrected" for the Martian atmosphere [e.g., *Bibring et al.*, 1990; *Erard et al.*, 1991; *Murchie et al.*, 1993; *Mustard et al.*, 1993]. This removal of the atmospheric signature from the surface reflectance, however, is not a straightforward task and can be misleading with regard to the spectral content of the Martian surface. The contribution of atmospheric water vapor

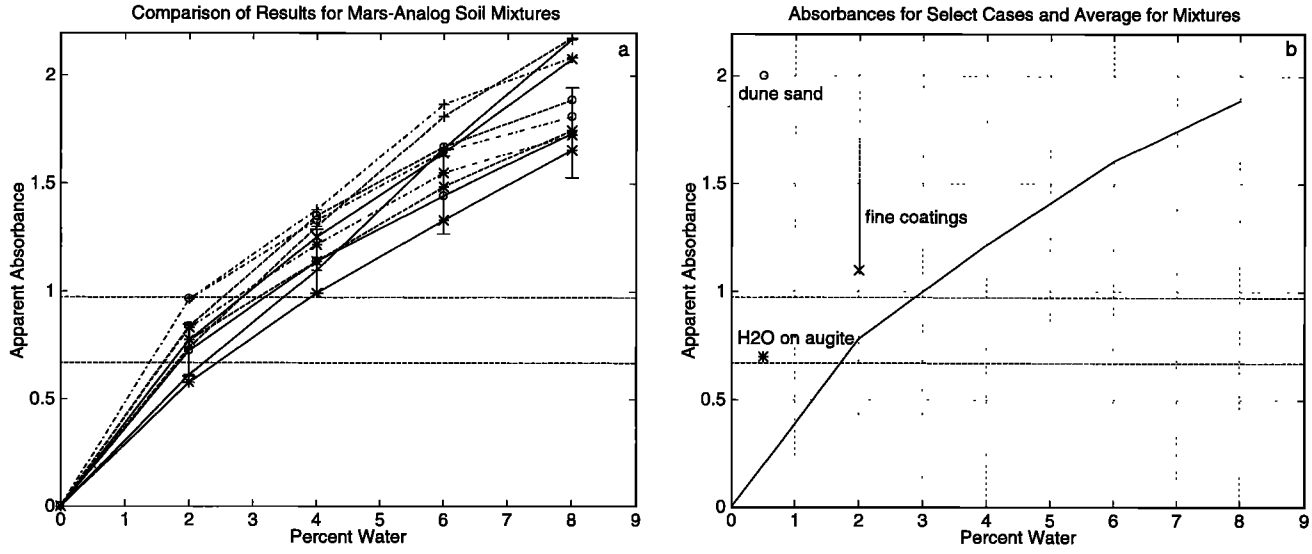

Figure 4. (a) Plot of apparent absorbances extracted from curves shown in Figure 3 and similar mixtures using plagioclase feldspar and augite as the anhydrous phase. Solid lines represent basalt, dashed lines are feldspar, and dash-dot lines are augite; asterisks represent palagonite; pluses are bentonite; circles are gypsum; and crosses are goethite. Horizontal lines at 0.67 and 0.97 represent the range of absorbances for the Martian surface calculated from ISM data (see text). Representative error bars are shown on the gypsum-basalt mixture. (b) Average apparent absorbance versus water content based on the curves from Figure 4a. Data points for adsorbed water on augite, reduced particle sizes for the hydrated phases in the mixtures, and hydrated coatings are shown for comparison.

to the surface signature is difficult to establish because an extremely weak feature at 2.544 μm provides the only constraint [*Erard et al.*, 1991]. The primary difficulty with the atmospheric correction, however, is due to a strong CO_2 absorption (centered at ~2.75 μm) which overlaps the short wavelength range of the surface hydration feature. Because this band never exceeds 85% on account of saturation attributed to stray light and atmospheric scattering [*Bibring et al.*, 1990; *Erard et al.*, 1994; *Erard and Calvin*, 1997], complete removal of the CO_2 contribution is nearly impossible to achieve.

The challenges associated with atmospheric correction are apparent from published surface spectra, which are not consistent across various papers. For example, one "corrected" curve for Isidis Planitia [*Mustard et al.*, 1993] has a band depth approximately 40% larger than previously published reductions of ISM spectra for the same region of Mars [*Erard et al.*, 1991]. J. Mustard (personal communication, 1997) indicated that absolute calibration of the 3-μm region of the spectra was not a primary goal of his paper and that owing to saturation of the 2.7-μm CO_2 band, the processed data are correlated with altitude (which indicates an inaccurate removal). Mustard is confident in the relative accuracy of his plots but suggested that curves from *Erard et al.* [1991] should be used for direct comparisons with laboratory data. The *Erard et al.* [1991] work, however, is a "first results" paper that had not incorporated more sophisticated atmospheric removal algorithms (S. Erard, personal communication, 1997). Which calibration, then, should be used to compare against the laboratory data?

Recent work by Murchie et al. (submitted manuscript, 1997) provides scatterplots of 3-μm band depths for the entire ISM data set. The absolute calibration of wavelengths larger than 2.6 μm in this work is tied to ISM observations of Phobos, which is nearly featureless in this range. Murchie et al. determined band depths by comparing the continuum level at 2.5 μm to an average of the signal strengths at 2.95, 3.00, and 3.05 μm, which specifically excludes the regions of the strongest CO_2 absorptions. The results range from approximately 0.49 to 0.62 with a large concentration of points around 0.59. This range for the 3-μm band depths corresponds to apparent absorbance values between 0.67 and 0.97 (with a large fraction of the points around 0.89) for the ISM data set. These absorbance values are consistent with the ones we calculated from individual, corrected spectra that we obtained directly from S. Erard: Amazonis Planitia (0.94), Eos Chasmata (0.74), Lunae Planum (0.97), and Syrtis Major (0.69). This range of apparent absorbance (0.67–0.97) will be used for comparison with the laboratory results and is shown in Figure 4.

3.2. Upper Limit for Water Content

Figure 4a shows a roughly linear increase in apparent absorbance as a function of water content. Departures from true linearity are likely due to incomplete modeling of scattering and diffuse reflectance by a simple logarithmic function. Regardless of the nonlinearity, these curves establish a reproducible relationship between the size of the absorbance and the water content for plausible mixtures of Martian surface materials and provide a reasonable data set for comparison against the spacecraft data. Since the magnitude and shape of the curves for the 10 different mineral mixtures are roughly the same (close to the uncertainties of the experiment), the apparent absorbance does not appear to have a strong dependence on the choice of the Mars-analog minerals in the mixture. On the basis of the average curve through the data (Figure 4b), we believe the upper limit for the water content of the Martian soil to be 4% by weight.

This value, which is based on the maximum absorbance in the ISM data, is judged to be conservative for two reasons. First, the particle size distributions of the hydrated and the dry

components of the mixtures that we used are approximately the same. In a natural environment the smallest particles will likely be dominated by phyllosilicates, since the weakly bound layers are easy to disrupt by physical weathering processes. Experiments using the minerals described above but with the hydrated phase limited to particles smaller than 35 μm resulted in apparent absorbances larger than 1.1 with only 2% water (see Figure 4b for comparison with nominal results). Small hydrated particles coating the surfaces of anhydrous scattering centers provide even greater opportunities for incident photons to be absorbed at 3 μm. In the limit where the hydrated phase is a coating rather than individual particles observable with an optical microscope, large absorbances can be achieved with minimal quantities of water. For example, an analysis of sands from the Kelso Dunes in the Mojave Desert, California, shows an apparent absorbance of greater than 2.0 for only 0.5% water (see Figures 5 and 4b). These 250- to 500-μm-diameter sand particles consist of quartz, feldspar, and amphibole, among other minerals [*Sharp*, 1966], and are coated by fine-grained clay minerals which enhance the 3-μm absorption. Hydrated coatings or "rinds" around surface particles are consistent with models of Martian soils [e.g., *Murchie et al.*, 1993].

Second, we found it difficult to "hide" quantities of water larger than 4% in the laboratory samples while maintaining the use of plausible mineral and size mixtures. It is, of course, possible to use fine particles of highly absorbing, but uncommon, materials to coat larger grains of hydrated phases to conceal large quantities of water. For example, experiments show that 1-μm particles of graphite coating 100-μm gypsum grains will yield an apparent absorbance of <0.4 for ~15% water by weight. The absolute reflectivities of Mars, however, are not consistent with an abundance of highly absorbing mineral phases. Our experiments with basalt and augite are already on the "dark" end of realistic visible albedoes, with values between 10% and 15%. Experiments using these dark, but plausible, particles coating larger hydrated sulfate grains were insufficient to mask the strong OH signature. Thus the particle size distributions and minerals used in our experiments allow us to conclude that the water content of the Martian soil is likely to be less than 4% by weight.

3.3. Spectral Shapes

In addition to providing constraints on the water content, the 3-μm surface absorption feature contains information about the composition of the hydrated phases in the Martian soil. For example, montmorillonite has a characteristic peak at approximately 2.76 μm [*van der Marel and Beutelspacher*, 1976]. Palagonite lacks this peak and exhibits a much more abrupt entrance into the short-wavelength end of the absorption feature when compared with gypsum. Unfortunately, these diagnostic compositional characteristics of candidate Martian minerals are concentrated in the short-wavelength end of the 3-μm absorption feature. The difficulties with atmospheric correction result in the greatest uncertainties occurring in this part of the spectrum and prevent the determination of surface composition from the 3-μm spectral shape.

One statement about spectral shape, however, can be made with relative confidence on the basis of our laboratory data: We can exclude goethite as the dominant hydrated mineral phase in the soil because its spectral peak for OH is at 3.18 μm (see Figure 3d), while the peak of the Mars absorption is unlikely to be at wavelengths longer than 3.0 μm [e.g., *Erard and Calvin*, 1997]. This constraint on the peak location in the Mars data is independent of the atmospheric correction because it relies primarily on data outside the CO_2 absorption.

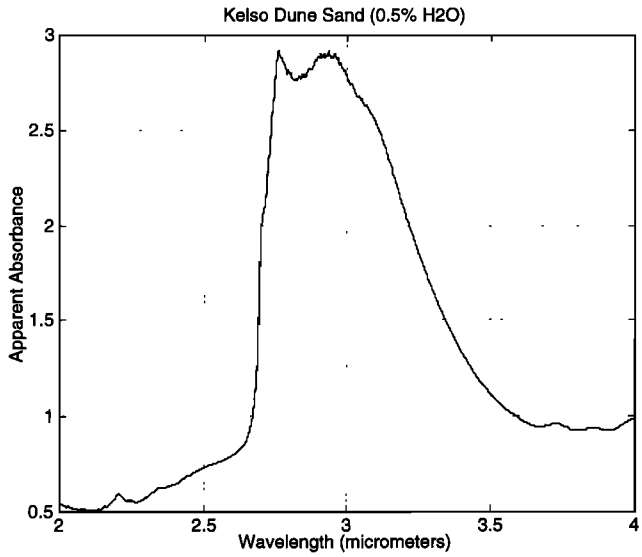

Figure 5. Apparent absorbance spectrum from Kelso Dunes sands. Thermal analyses indicate approximately 0.5 wt % water in these samples. This figure shows that absorbance values substantially larger than the range evident in the ISM data can be obtained with very small quantities of water when small particles of hydrous minerals coat larger anhydrous grains.

3.4. Liquid, Frozen, and Adsorbed Water

One could argue that the origin of the feature in the ISM data is not necessarily associated with water bound in a hydrated mineral but rather could be due to liquid, frozen, or adsorbed water at the surface. Each of these options, however, is unlikely to be responsible for the entire absorption feature. Because of the low water vapor pressure in the atmosphere (on the order of a microbar), liquid water with or without brines is not stable at the Martian surface. In the season ($Ls \sim 10°$) and latitude ($L \sim 10°$N) of these Phobos 2 daylight observations (0900–1600 LT), frost is not likely to be at the surface [e.g., *Ingersoll*, 1970; *Jakosky*, 1985]. Furthermore, the peak location (~3.07 μm) of the water ice absorption feature is at a longer wavelength than the peak in the spacecraft data.

Some amount of adsorbed water in equilibrium with the atmosphere, however, should be present on the soil grains at the Martian surface. We conducted experiments to determine absorption depths from water adsorbed on anhydrous particles. Only the smallest grains (<35 μm) were used so surface area could be maximized, and the samples were exposed to high humidity immediately prior to obtaining the infrared spectra. Augite samples yielded apparent absorbances of approximately 0.7, and a thermal analysis of these samples showed that they contained ~0.5 wt % water (see Figure 4b for comparison with other laboratory results). This apparent absorbance is at the low end of the absorbance values derived from the ISM data set. This indicates that at saturation in room temperature, a collection of angular (rough) anhydrous grains substantially smaller than the mean particle size of the Martian soil still has insufficient surface area to hold a quantity of adsorbed water that could completely reproduce the ISM spectra. Under Martian conditions a recent model indicates that

palagonite with a specific surface area of 17 $m^2 g^{-1}$ (consistent with an estimate by *Ballou et al.* [1978] for the Martian soil) would hold less than 0.04% adsorbed water [*Zent and Quinn*, 1997]. This quantity of water would have a much smaller absorbance than is evident from the spacecraft data and is further evidence that adsorbed water cannot be responsible for the entire 3-μm feature. In addition, the GC-MS evolved much of its water at temperatures above 350°C [*Biemann et al.*, 1977]. Even for the rapid heating steps (<30 s) utilized by the instrument, most of the adsorbed water should have been released at lower temperatures.

3.5. Implications and Predictions

Using plausible constituents and particle sizes for the Martian soil, we believe that the Martian surface fines contain at most 4% water by weight. This conclusion does not imply, however, that Mars never had a large supply of hydrated mineral phases. It only addresses the abundance of hydrated minerals present at the immediate surface today. Desiccation processes resulting from the low partial pressure of water vapor, and possibly from radiation-induced dehydration active over geologic timescales, could have decomposed an initial supply of hydrated phases into anhydrous products.

In principle, an abundance of hydrated phases could still be present beneath the micrometer level depths sampled by the ISM instrument and beneath the 10-cm depths accessed by the robotic collection arm of the Viking landers. The January 1999 launch of the Mars Surveyor lander offers opportunities to test our conclusions. The current design concept for the New Millennium Mars microprobes, which will be carried "piggyback" on this mission, features an evolved water analysis instrument to search for hydration ~1 m beneath the surface. In addition, the thermal and evolved gas analyzer (TEGA) on the lander itself is intended to carry out the first in situ mineralogical analysis of the Martian surface. It should have good sensitivity for bound water in soil minerals. The sampling arm is likely to be able to dig at least as deep as the Viking arm. Our interpretation of the laboratory results described in this paper leads us to expect that this mineralogy experiment will find less than 4% water adsorbed or bound in samples obtained from the upper few centimeters of the surface. TEGA should also be able to identify the phase(s) in which the water is contained. The Surveyor lander will land near the Martian south pole in early southern spring, and this prediction does not include any water that may be contained as ice or frost.

4. Conclusions

1. On the basis of laboratory simulations of the 3-μm absorption feature, we believe that the surface of Mars contains a maximum of 4% water adsorbed and/or bound in the surface minerals. These results are consistent with the in situ measurements of evolved water performed by the gas chromatograph–mass spectrometer instrument on the Viking landers and indicate a drier, more dehydrated soil than is implied by much modeling of early Mars conditions.

2. The shape of the short-wavelength portion of the 3-μm absorption feature is highly uncertain in Mars spectra owing to complexities in removal of the atmospheric CO_2 and water vapor. Goethite, however, can be excluded as a major component of the soil because its peak location is at longer wavelengths than the spacecraft data suggests and is in a region of the spectrum that is not affected by the atmosphere. Small amounts of dehydrated palagonite, hydrated sulfates such as gypsum, and poorly crystalline clays cannot be excluded on the basis of the existing 3-μm reflection spectra of Mars.

3. Large apparent absorbances (>0.7) can be achieved with relatively small quantities of water (~0.5%) physically adsorbed on the surfaces of anhydrous mineral grains. The evolution of water between 350°C and 500°C in the Viking lander GC-MS indicates that adsorbed water is not the only form of hydration in the soil.

4. Our interpretation of the laboratory data leads us to expect that the TEGA mineralogy experiment on board the Mars Surveyor lander and the evolved water experiment on the accompanying microprobes will find less than 4% water adsorbed or bound in minerals in the Martian soil.

Acknowledgments. We thank Wendy Calvin and Scott Murchie for thorough reviews and helpful discussions which have greatly improved this manuscript. Stephane Erard provided us with digital versions of ISM spectra for comparison with our laboratory data. Aaron Zent provided the Pahala Ash, and Lazlo Keszthelyi collected the basalt samples for our experiments. Albert Yen acknowledges the support of the NASA Graduate Student Researchers Program. George Rossman acknowledges the support of NSF EAR 9218980.

References

Allen, C. C., J. L. Gooding, M. Jercinovic, and K. Keil, Altered basaltic glass: A terrestrial analog to the soil of Mars, *Icarus*, *45*, 347–369, 1981.

Anderson, D. M., and A. R. Tice, The analysis of water in the Martian regolith, *J. Mol. Evol.*, *14*, 33–38, 1979.

Arvidson, R. E., J. L. Gooding, and H. J. Moore, The Martian surface as imaged, sampled, and analyzed by the Viking landers, *Rev. Geophys.*, *27*, 39–60, 1989.

Baird, A. K., A. J. Castro, B. C. Clark, P. Toulmin III, H. Rose Jr., K. Keil, and J. L. Gooding, The Viking X Ray Fluorescence Experiment: Sampling strategies and laboratory simulations, *J. Geophys. Res.*, *82*, 4595–4624, 1977.

Ballou, E. V., P. C. Wood, T. Wydeven, M. E. Lehwalt, and R. E. Mack, Chemical interpretation of Viking lander 1 Life Detection Experiment, *Nature*, *271*, 644–645, 1978.

Banin, A., B. C. Clark, and H. Wanke, Surface chemistry and mineralogy, in *Mars*, edited by H. H. Kieffer et al., pp. 594–625, Univ. of Ariz. Press, Tucson, 1992.

Banin, A., T. Ben-Shlomo, L. Margulies, D. F. Blake, R. L. Mancinelli, and A. U. Gehring, The nanophase iron mineral(s) in Mars soil, *J. Geophys. Res.*, *98*, 20,831–20,853, 1993.

Bell, J. F., III, R. V. Morris, and J. B. Adams, Thermally altered palagonitic tephra: A spectral and process analog to the soil and dust of Mars, *J. Geophys. Res.*, *98*, 3373–3385, 1993.

Bibring, J. P., et al., ISM observations of Mars and Phobos: First results, *Proc. Lunar Planet. Sci. Conf.*, *20th*, 461–471, 1990.

Biemann, K., et al., The Search for organic substances and inorganic volatile compounds in the surface of Mars, *J. Geophys. Res.*, *82*, 4641–4658, 1977.

Bishop, J. L., C. M. Pieters, and R. G. Burns, Reflectance and Mossbauer spectroscopy of ferrihydrite-montmorillonite assemblages as Mars soil analog materials, *Geochim. Cosmochim. Acta*, *57*, 4583–4595, 1993.

Burns, R. G., Gossans on Mars, *Proc. Lunar Planet. Sci. Conf.*, *18th*, 713–721, 1988.

Burns, R. G., and D. S. Fisher, Rates of oxidative weathering on the surface of Mars, *J. Geophys. Res.*, *98*, 3365–3372, 1993.

Calvin, W. M., Variation of the 3-mm absorption feature on Mars: Observations over eastern Valles Marineris by the Mariner 6 infrared spectrometer, *J. Geophys. Res.*, *102*, 9097–9107, 1997.

Carr, M. H., *Water on Mars*, 229 pp., Oxford Univ. Press, New York, 1996.

Clark, R. N., and T. L. Roush, Reflectance spectroscopy: Quantitative analysis techniques for remote sensing applications, *J. Geophys. Res.*, *89*, 6329–6340, 1984.

De Bruyn, C. M. A., and H. W. van der Marel, Mineralogical analysis of soil clays, *Geol. Mijnbouw*, *16*, 69–83, 1954.

Erard, S., and W. Calvin, New composite spectra of Mars, 0.4–5.7 μm, *Icarus*, *130*, 449–460, 1997.

Erard, S., J. P. Bibring, J. Mustard, O. Forni, J. W. Head, S. Hurtrez, Y. Langevin, C. M. Pieters, J. Rosenqvist, and C. Sotin, Spatial variations in composition of the Valles Marineris and Isidis Planitia regions of Mars derived from ISM data, *Proc. Planet. Sci. Conf., 21st*, 437–455, 1991.

Erard, S., J. Mustard, S. Murchie, J. P. Bibring, P. Cerroni, and A. Coradini, Martian aerosols: Near-infrared spectral properties and effects on the observation of the surface, *Icarus*, *111*, 317–337, 1994.

Gooding, J. L., and K. Keil, Alteration of glass as a possible source of clay minerals on Mars, *Geophys. Res. Lett.*, *5*, 727–730, 1978.

Greeley, R., N. Lancaster, S. Lee, and P. Thomas, Martian aeolian processes, sediments, and features, in *Mars*, edited by H. H. Kieffer et al., pp. 730–766, Univ. of Ariz. Press, Tucson, 1992.

Hapke, B., *Theory of Reflectance and Emittance Spectroscopy*, pp. 318–324, Cambridge Univ. Press, New York, 1993.

Houck, J. R., J. B. Pollack, C. Sagan, D. Schaack, and J. A. Decker Jr., High-altitude infrared spectroscopic evidence for bound water on Mars, *Icarus*, *18*, 470–480, 1973.

Ingersoll, A. P., Mars: Occurrence of liquid water, *Science*, *168*, 972–973, 1970.

Jakosky, B. M., The seasonal cycle of water on Mars, *Space Sci. Rev.*, *41*, 131–200, 1985.

Kortum, G., *Reflectance Spectroscopy*, 366 pp., Springer-Verlag, New York, 1969.

Moroz, V. I., The infrared spectrum of Mars (1.1–4.1 μm), *Astron. Zh.*, *41*, 350, 1964.

Morris, R. V., H. V. Lauer Jr., J. L. Gooding, and W. W. Mendell, Spectral evidence and implications for the occurrence of aluminous iron oxides on Mars, in *Abstracts of Papers Submitted to the Fourteenth Lunar and Planetary Science Conference*, part 2, pp. 526–527, Lunar and Planetary Inst., Houston, Tex., 1983.

Morris, R. V., J. L. Gooding, H. V. Lauer Jr., and R. B. Singer, Origins of Marslike spectral and magnetic properties of a Hawaiian palagonitic soil, *J. Geophys. Res.*, *95*, 14,427–14,434, 1990.

Murchie, S., J. Mustard, J. Bishop, J. Head, C. Pieters, and S. Erard, Spatial variations in the spectral properties of bright regions on Mars, *Icarus*, *105*, 454–468, 1993.

Mustard, J. F., S. Erard, J. P. Bibring, J. W. Head, S. Hurtrez, Y. Langevin, C. M. Pieters, and C. J. Sotin, The surface of Syrtis Major: Composition of the volcanic substrate and mixing with altered dust and soil, *J. Geophys. Res.*, *98*, 3387–3400, 1993.

Palluconi, F. D., and H. H. Kieffer, Thermal inertia mapping of Mars from 60°S to 60°N, *Icarus*, *45*, 415–426, 1981.

Pimentel, G. C., P. B. Forney, and K. C. Herr, Evidence about hydrate and solid water in the Martian surface from the 1969 Mariner infrared spectrometer, *J. Geophys. Res.*, *79*, 1623–1634, 1974.

Pollack, J. B., D. S. Colburn, F. M. Flasar, R. Kahn, C. E. Carlston, and D. C. Pidek, Properties and effects of dust particles suspended in the Martian atmosphere, *J. Geophys. Res.*, *84*, 2929–2945, 1979.

Sharp, R. P., Kelso Dunes, Mojave Desert, California, *Geol. Soc. Am. Bull.*, *77*, 1045–1074, 1966.

Sharp, R. P., and M. C. Malin, Surface geology from Viking landers on Mars: A second look, *Geol. Soc. Am. Bull.*, *95*, 1398–1412, 1984.

Singer, R. B., Spectral evidence for the mineralogy of high-albedo soils and dust on Mars, *J. Geophys. Res.*, *87*, 10,159–10,168, 1982.

Sinton, W. M., On the composition of Martian surface materials, *Icarus*, *6*, 222–228, 1967.

Soderblom, L. A., and D. B. Wenner, Possible fossil H_2O liquid-ice interfaces in the Martian crust, *Icarus*, *34*, 622–637, 1978.

Toulmin, P., III, A. K. Baird, B. C. Clark, K. Keil, H. J. Rose Jr., R. P. Christian, P. H. Evans, and W. C. Kelliher, Geochemical and mineralogical interpretation of the Viking inorganic chemical results, *J. Geophys. Res.*, *82*, 4625–4634, 1977.

van der Marel, H. W., and H. Beutelspacher, *Atlas of Infrared Spectroscopy of Clay Minerals and Their Admixtures*, pp. 249–253, Elsevier Sci., New York, 1976.

Zent, A. P., and R. C. Quinn, Measurement of H_2O adsorption under Mars-like conditions: Effects of adsorbent heterogeneity, *J. Geophys. Res.*, *102*, 9085–9095, 1997.

Zolotov, M. Y., Y. I. Sidorov, V. P. Volkov, M. V. Borisov, and I. L. Khodakovsky, Mineral composition of Martian regolith: Thermodynamic assessment, in Abstracts of Papers Submitted to the Fourteenth Lunar and Planetary Science Conference, part 2, pp. 883–884, Lunar and Planet. Inst., Houston, Tex., 1983.

B. C. Murray, G. R. Rossman, and A. S. Yen, Division of Geological and Planetary Sciences, Mail Code 150-21, California Institute of Technology, Pasadena, CA 91125. (e-mail: ayen@gps.caltech.edu)

(Received June 13, 1997; revised February 27, 1998;
accepted March 5, 1998.)